Mesoporous Carbon Materials as Electrodes for Electrochemical Supercapacitors

F. Lufrano[*]*, P. Staiti*

CNR-ITAE, Istituto di Tecnologie Avanzate per l'Energia "Nicola Giordano"
Via Salita S. Lucia, 5 – 98126 Messina, Italy
[*]E-mail: lufrano@itae.cnr.it

In this paper, we report the synthesis and characterization of mesoporous carbons, which were obtained using SBA-15 silica as the template material and sucrose as the carbon source. The prepared silica template and mesoporous carbons were characterized by nitrogen adsorption-desorption, low angle X-ray diffraction (XRD) and transmission electron microscopy (TEM). Synthesized carbons were used to prepare composite electrodes for solid-state supercapacitors. The electrochemical characteristics of mesoporous carbons in supercapacitors were studied by cyclic voltammetry and electrochemical impedance spectroscopy. The study showed that a value of specific capacitance of 132 F g^{-1} (for a single electrode) was obtained with the CMK-3A mesoporous carbon, which was 68% higher than that of an activated carbon that was used as a reference material. The superior performance was 127% (12.05 µF cm^{-2} vs. 5.3 µF cm^{-2}) when the double-layer capacitance of the mesoporous carbon was compared to that of the reference carbon. These findings for the mesoporous carbon-based supercapacitor were explained on the basis of a high pseudo-capacitance and other physico-chemical properties of this carbon, such as the pore structure, accessibility of pores to the electrolyte, and surface wettability by surface functional groups. All of these properties were improved compared to those of the activated carbon.

1. INTRODUCTION

Supercapacitors are electrochemical energy storage devices that provide high power density and remarkable energy. These characteristics are of increasing interest for energy storage applications such as: electric vehicles, backup power systems, and electronic components. They are based on a storage mechanism that results from the formation of an electric double layer at the interface between an electronically conductive material and an electrolyte solution [1-3]. A typical supercapacitor is

formed from two carbon electrodes and a liquid electrolyte supported in a porous matrix (separator) interposed between the electrodes. The energy stored in a carbon-based supercapacitor is principally a function of the following parameters: the specific surface area and pore structure of electrodes, the ionic conductivity, and the voltage stability of the electrolyte. Therefore, typical materials used in conventional electrodes must have a high surface area, such as activated carbons [1-6], carbon fibers [7,8], and carbon aerogels [9-10]. The electrolytes generally used in supercapacitors are aqueous solutions of H_2SO_4 or KOH [1-3, 6, 11] or non-aqueous solutions of tetraethyl-ammonium tetrafluoroborate (ET_4NBF_4) in organic solvents [1-5, 11-13]. The introduction of solid polymer electrolytes in supercapacitors, which are used as an alternative to liquid electrolytes, may provide a number of advantages. Advantages from the technological point of view are a more flexible structure, a more compact geometry, and easier packaging. And, an advantage from the management point of view is a safer device that is free from leakages of corrosive and dangerous liquids.

Therefore, recently we have focused our research efforts on the introduction of Nafion-based polymer electrolytes for the development of solid-state supercapacitors [14-17]. The Nafion electrolyte is well known to have high ion conductivity ($> 5 \cdot 10^{-2}$ $S \cdot cm^{-1}$ at R.T.), excellent mechanical strength, as well as remarkable chemical and electrochemical stability. Furthermore, since Nafion is readily available in ionomer solution it can be advantageously used for the preparation of composite electrodes, in which Nafion functions both as the binder of carbon particles and, of the polymer electrolyte. The advantage derived from distributing the polymer electrolyte in the electrodes is determined by the enlargement of the electrode/electrolyte interface that increases the fraction of carbon taking part in the charging process, thus improving specific capacitance.

We believe that if carbon materials with a high specific surface area and with a well defined pores structure are used, well engineered solid-state supercapacitors can deliver as much energy and power density as those equipped with liquid electrolyte-based supercapacitors with the advantage of the design and realization of lightweight and flexible devices. Recently, new types of carbons known as nanostructured mesoporous carbons have been of interest as materials in the negative electrodes of rechargeable lithium batteries [18] and as active carbon materials of supercapacitor electrodes [13, 19-20]. It has been shown in the literature that the performances of battery and/or supercapacitor electrodes were negatively influenced by mass transport limitations due to the small ion mobility of the electrolyte into the carbon pores. For example, Tamai et al. [21] reported that the use of carbon with prevailing mesoporosity in the electrodes allowed the improvement of the specific capacitance of carbon-based supercapacitors. Yamada et al. [22] compared different carbons of comparable specific surface areas and with different pore size distributions and showed that those that were mostly mesoporous had a higher capacitance. Moreover, Yoon et al. [23] demonstrated that the carbons with higher fraction of mesopores supplied higher current densities and, showed a smaller time constant (RC) with respect to mainly microporous carbons. However, these studies were performed on liquid electrolyte-based supercapacitors [21-23], and it is likely that the micro-structural features of such carbon materials could exert an even greater influence on the development of efficient polymer electrolyte-based supercapacitors. In the 1999, the first nanostructured mesoporous carbons were synthesized by Ryoo et al. [24] starting from mesoporous silica templates (MCM-48) filled with sucrose as carbon source. Subsequently, the same group reported the synthesis of mesoporous carbons

using a different type of silica, SBA-15 as a template material [25]. The carbon obtained, which was called CMK-3, was a perfect replica of the SBA-15 silica template. The structure of this carbon material consisted of rods arranged in a hexagonal structure in which bridges between parallel rods allowed the stabilization of the structure.

Here, we will report the synthesis of mesoporous nano-structured carbons using mesoporous silica, SBA-15, as the template and sucrose as the carbon source and demonstrate their use in the preparation of composite electrodes and the fabrication of small scale solid-state supercapacitors.

Furthermore, we also report research on the influence of the properties of carbon materials, modified by thermal treatments and on the capacitance performances of different supercapacitors. The assessments of the electrochemical characteristics were performed by cyclic voltammetry (CV) and electrochemical impedance spectroscopy (EIS).

The electrochemical performances of these mesoporous carbons were compared to those of a reference microporous activated carbon in order to establish the structural and surface characteristics of carbon materials that may influence the performance of solid-state supercapacitors.

2. EXPERIMENTAL

2.1. Synthesis of SBA-15 silica

Mesoporous carbons were prepared by using silica as a hard template. The silica template, SBA-15, was synthesized using a procedure similar to that reported by Zhao [26]. In particular, 20 g of the triblock copolymer of poly(ethylene glycol)$_{20}$-block-poly(propylene glycol)$_{70}$-block-poly(ethylene glycol)$_{20}$ (EO$_{20}$PO$_{70}$EO$_{20}$ (average MW = 5800 Da, Aldrich) was dispersed in 150 ml of H$_2$O, followed by the addition of 580 ml of 2 M HCl. The resulting solution was stirred at 35 °C in a 3-necked round bottom flask until a clear solution was obtained. Next, 43.4 g of tetraethoxysilane (TEOS) was added under stirring at 35 °C for 20 hours and after is still maintained at 100 °C for 24 h. The precipitate was filtered, dried at ambient temperature, and calcined in air at 500 °C for 6 h.

2.2. Synthesis of mesoporous CMK-3 carbon

Mesoporous carbons were prepared using the SBA-15 silica template following the procedure described by Jun et al. [25]. In a typical synthesis, 30 g of H$_2$O, 0.86 g of H$_2$SO$_4$ conc., and 7.65 g of sucrose were homogenized in a beaker by stirring. This dispersion was added dropwise to 6.02 g of SBA-15 silica. The impregnated silica sample, was first heated in oven at 100 °C for 6 h, and then at 160 °C for 6 additional hours. This step was repeated a second time adding 30 g of H$_2$O, 0.54 g of H$_2$SO$_4$, and 4.8 g of sucrose. After thermal treatment at 160 °C, the material was divided in two portions which were pyrolyzed in a quartz tube under helium at 850 and 900 °C. Finally, the silica template was removed by treatment with a 1.5 M NaOH solution (50 vol% ethanol, 50 vol% H$_2$O) at 70 °C. The carbon samples pyrolyzed at 850 and 900 °C were designated CMK-3A and CMK-3B, respectively.

2.3. Physical and structural characterization of mesoporous carbons

Nitrogen adsorption-desorption measurements were performed at 77 k with a Sorptomatic model 1990 (ThermoQuest, Milan – Italy). Before measurements were made, all samples were degassed at 250 °C under vacuum for at least 3 h.

The specific surface area (SSA) of carbons was determined by the Brunauer-Emmett-Teller (BET) method in the P/P_0 range from 0.05 to 0.20, whereas the total pore volume was calculated at a relative pressure of $P/P_0 = 0.95$. A comparatively high-resolution α_S-plot was used as a second method for the assessment of the SSA. The α_S-plot of a nonporous carbon black, Cabot BT 280 [28], was used as the standard isotherm. The mesopore pore size distribution (PSD) was obtained by the Barrett-Joyner-Halenda (BJH) method, which was applied to the desorption branch of the isotherms [29].

Powder x-ray diffraction measurements were performed using a Philips X'Pert PRO diffractometer using Cu Kα radiation (wavelength = 0.15418 nm), while transmission electron microscope (TEM) images were collected with a PHILIPS CM12 instrument.

2.4. Preparation of the composite electrodes

The electrodes for the supercapacitor were prepared by a casting method, which consisted of spreading a slurry of the carbon material, Nafion ionomer, graphite fibers, and N,N–dimethylacetamide (DMAc) on a glass plate. After casting the electrodes, they were detached from the plate and treated at 120 °C for 1 hour and at 160 °C for 20 minutes. The composition of the electrodes prepared was 45 wt.% carbon, 50 wt.% of Nafion, and 5 wt.% graphite fibers. Two different electrodes were prepared with the CMK-3A and the CMK-3B carbons. The loading of CMK-3A and CMK-3B carbons on both electrodes was 4.7 ± 0.2 mg cm^{-2} and their thickness was 150 ± 20 μm. An electrode with 8 mg cm^{-2} of activated carbon, Norit A Supra Eur (NASE, Norit Italia S.p.A. Ravenna – Italy), was prepared with the same procedure and used for comparison.

2.5. Preparation of the membrane and electrodes assemblies and electrochemical characterization

The supercapacitors were obtained by contacting the faces of two 4 cm^2 electrodes with a 5 cm^2 Nafion 115 membrane (DuPont). The assemblies were realized by hot pressing the sandwich at 100 kg cm^{-2}, at 130 °C for 10 minutes.

The electrochemical measurements on supercapacitors were performed using cyclic voltammetry (CV) at different scan rates that ranged from 5 to 40 mV s^{-1}, in the voltage range of 0–1 V, using an AMEL apparatus (AMEL S.r.l. Milan, Italy). The specific capacitance, C_s, obtained from cyclic voltammetry was calculated by $C_s=[4(I/(dV/dt))/m]$; where I is the current in amperes, dV/dt is the voltage scan rate in V/s, and m is the mass in grams of the active carbon material. The number 4 is necessary in order to report the capacitance of a single electrode. The electrochemical impedance spectroscopy (EIS) measurements were performed using a Potentiostat PGSTAT 30 (Autolab, Ecochemie, Netherlands) with a FRA2 module at frequencies 1 mHz to 10 MHz.

3. RESULTS AND DISCUSSION

3.1. Physico-chemical characterization of mesoporous carbons.

The porous structure of prepared carbons was determined by nitrogen adsorption measurements. Figure 1 shows the nitrogen adsorption-desorption isotherms of mesoporous CMK-3A and CMK-3B carbons and isotherms of commercial activated carbon (Norit A Supra Eur (NASE) that was used as the reference material. The isotherms of CMK-3A and CMK-3B are type-IV curves with a capillary condensation step and a slight hysteresis loop at relative pressures (P/P_0) at about 0.45, which is indicative of mesoporosity. In contrast, the NASE activated carbon instead shows a type-I isotherm that is characteristic of microporous material with a high volume of nitrogen adsorption at relative pressures $P/P_0 < 0.1$. The values of N_2 sorption at $P/P_0 = 0.1$, which are 383, 282, and 184 cm^3 g^{-1} for NASE, CMK-3A, and CMK-3B carbons, respectively, indicate that these carbons are also microporous. The BET specific surface area, pore volume, and other textural properties of the carbons determined by nitrogen adsorption-desorption and XRD measurements are summarized in Table I.

Table 1. Pore properties of SBA-15 silica and mesoporous carbons.

Sample	S_{BET}[1] $(m^2 g^{-1})$	S, α_S (Kruk) $m^2 g^{-1}$	Vp[2] $(cm^3 g^{-1})$	V_{N2} (DR)[3] $(cm^3 g^{-1})$	Unit cell a_o[4] (nm)	Dp, BJH[5]
SBA-15	623	-	0.63	0.22	10.5	7.3[6]
CMK-3A	1120	1124	0.80	0.40	9.5	3.56
CMK-3B	765	763	0.70	0.27	9.38	3.58
NASE	1525	1500	0.78	0.56	-	1.9

1. Specific surface area determined by the BET method for P/P_0 from 0.05 to 0.2.
2. Total pore volume calculated at $P/P_0 = 0.95$.
3. Volume of micropores (< 2 nm) as determined by Dubinin-Radushkevich.
4. Unit cell parameter $a_o = 2 * d (100)/ (\sqrt 3)$ from XRD analysis.
5. Pores diameter (Dp) as determined by Barret-Joyner-Halenda (BJH) from desorption data.
6. Pores diameter (Dp) as determined by BJH from adsorption data.

The BET specific surface areas of the mesoporous carbons are 1120 and 765 $m^2 g^{-1}$ for CMK-3A and CMK-3B, respectively, while the respective total pore volumes at $P/P_0 = 0.95$ are 0.80 and 0.70 $cm^3 g^{-1}$. The BET surface area was 1525 $m^2 g^{-1}$ and the total pore volume ($P/P_0 = 0.95$) was 0.78 $cm^3 g^{-1}$ for the NASE carbon.

The inset in Figure 1 shows the pores size distributions (PSD) curves as determined by the BJH method. The PSD show well-defined peaks at pore diameter from 3.5 to 3.6 nm for CMK-3A and CMK-3B samples, whereas the NASE mainly has micropores, i.e., pores < 2 nm with low mesoporosity.
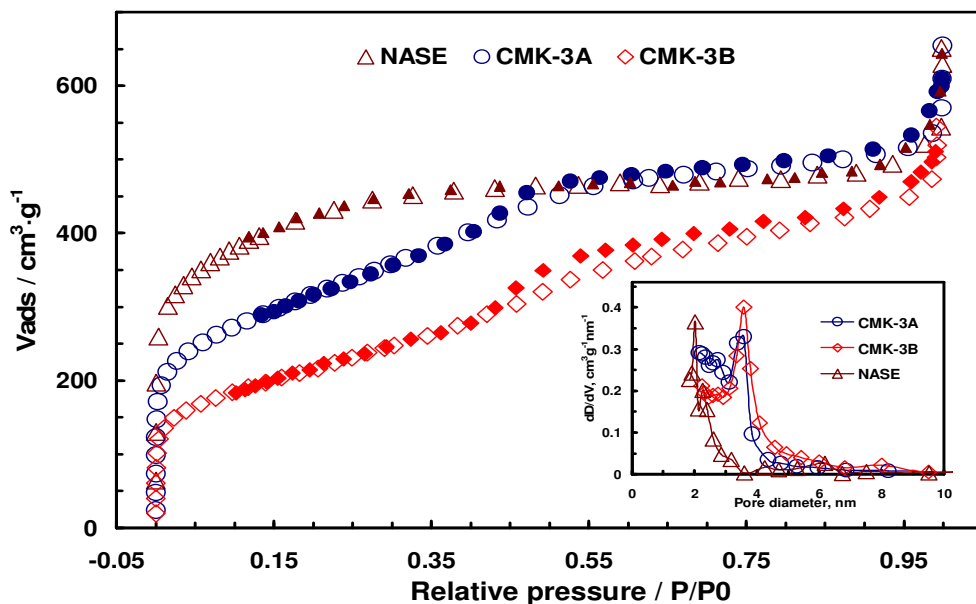

Figure 1. Nitrogen adsorption and desorption isotherms and pore size distributions (BJH method) of CMK-3A (calcined at 850°C), CMK-3B (calcined at 900°C) mesoporous carbons and NASE activated carbon.

CMK-3A and CMK-3B carbons also exhibit microporosity. This originated from the carbonization process of the sucrose and should be localized inside the carbon rods and/or in the spacers that connect the carbon rods and is in agreement with the results reported by Ryoo et al. [24]. The micropore volumes were 0.40 and 0.27 $cm^3 g^{-1}$ for CMK-3A and CMK-3B, respectively. These values, which are reported in Table I, are similar to those previously obtained by other authors [20, 30-31] for the same type of carbon. As has been previously shown, the amount of microporosity depends on the type of carbon source used in the impregnation step and on the temperature and conditions at which the syntheses were performed.

Figure 2 shows the TEM images of channels for the synthesized for CMK-3A carbon. Similar TEM images, which are not reported here, were also obtained from CMK-3B carbon (the carbon treated at 900 °C).
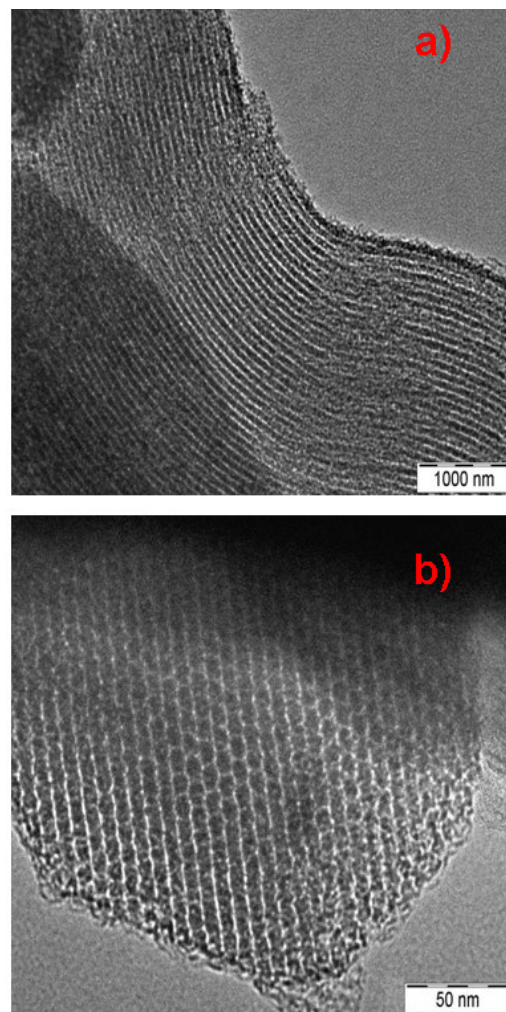
Figure 2. TEM images of CMK-3A carbon. a) frontal view of channels in CMK-3A carbon; b) lateral view of channels in CMK-3A carbon.

Figure 2a shows the characteristic structure of CMK-3A carbon with the channels arranged in a hexagonal structure. Figure 2b shows the channels in the of CMK-3A carbon from a point of view that is orthogonal to the channels.

The average diameters for the carbon rods may be seen to be about 7 nm; and an inter-axis distance of ~ 8.5 nm between two adjacent carbon rods may be measured. These values are in agreement with those originally reported by Jun et al. [25].

The presence of peaks in the XRD patterns at a low angle may be assigned to (100), (110), and (200) diffractions from 2-D symmetry associated with the hexagonal structure. The diffraction peaks (110) and (200) of SBA-15 silica are well-resolved, whereas those relative to CMK-3A carbon are less defined. The calculated values of d-spacing are 8.25 nm and 8.12 nm for the CMK-3A and CMK-3B carbons, respectively and are in agreement with those measured using the TEM images.
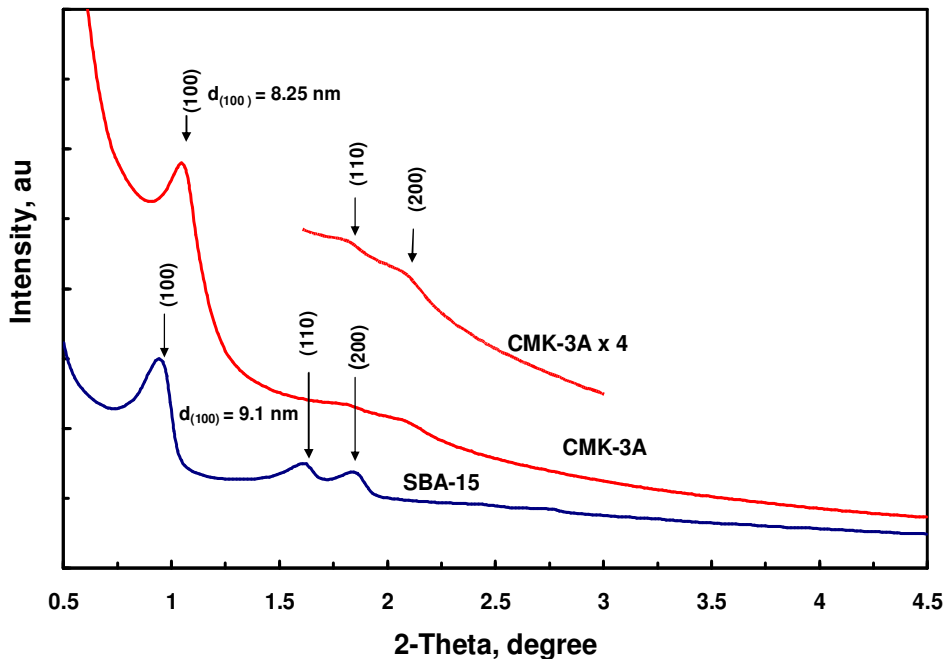
Figure 3. Small angle XRD diffraction patterns of and SBA-15 silica CMK-3A carbon.
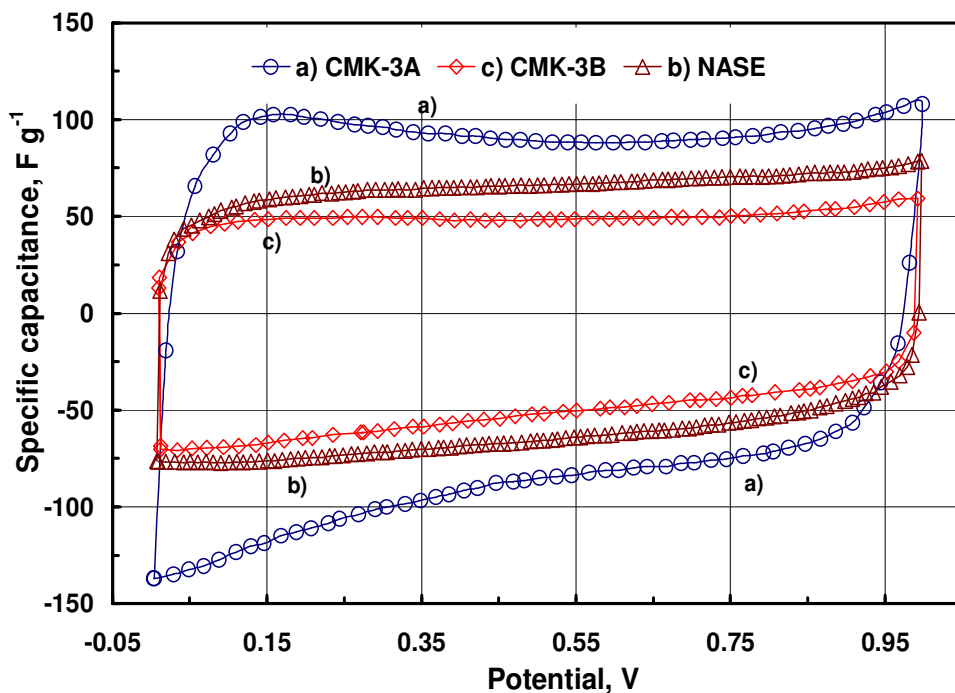

Figure 4. Cyclic voltammograms for different carbon supercapacitors. The specific capacitance referred to the weight of carbon materials in a single electrode. Voltage scan rate was 10 mV s^{-1}.

3.2. Cyclic voltammetry studies of carbon materials

Figure 4 shows the voltammograms of the carbons studied, in which the specific capacitance (C_s) of capacitor is reported as a function of cell voltage. The voltammograms show that the CMK-3A based supercapacitor exhibits a higher specific capacitance compared to those of NASE and CMK-3B carbons, notwithstanding the latter carbons have more rectangular shapes. The imperfect box-like capacitive behaviour of CMK-3A carbon-based supercapacitor for cell voltages from 0 to 0.3 V and viceversa is indicative of the presence of pseudo-capacitance due to redox process, and also shows a relatively high electronic resistance of this material. These aspect are likely due to a higher content of surface functional groups and lower degree of graphitization of CMK-3A carbon compared to than of NASE and CMK-3B carbons.

Generally, in the literature [32-33] the specific capacitance is reported to roughly increase linearly with the specific surface area (SSA) of the carbon material. However, such a trend sometimes shows different behavior in carbons with very high SSA and/or when non-aqueous electrolytes are used in the supercapacitors. In the former cases, i.e., with highly microporous carbons, it is likely that a fraction of pores (the smaller micropores) does not take part at the formation of the double layer because the electrolyte does not reach them. In the latter situation, it is probable that the capacitance performances [34-35] are controlled by ions sieving phenomena due to the dimension of the solvated ions of non-aqueous electrolyte. Moreover, some authors have attributed such effects to capacitance limitations, which are determined by space constriction, i.e., to the difficulty in accommodating the larger ions inside the pores of the carbon materials [34].

In this study, we report that the capacitance performance of CMK-3A, 132 F g^{-1}, is higher than that obtained with NASE activated carbon, 80.5 F g^{-1}. These values are in contrast with the expected trend versus the specific surface area. In fact, the SSA of NASE, which is 1525 m^2 g^{-1}, is higher than that of CMK-3A, which is 1120 m^2 g^{-1}, but the capacitance is higher for the latter material. In order to explain these results the fact that the NASE activated carbon is a highly microporous material (see Figure 1) should be taken into account as well as the fact that it was expected that a large fraction of its pores would not be available for the charging process.

Thus, the smallest micropores, which make the major contribution to the large specific surface area of activated carbons, could only provide a minor contribution to the electrical storage by double-layer capacitance. The lower double-layer capacitance of the CMK-3B, 7.3 μF cm^{-2}, compared to CMK-3A, 12.05 μF cm^{-2}, could be explained by the higher thermal treatment (900 °C) of the former carbon, which removes many of the functional groups present on the surface of carbon so that it becomes more hydrophobic and has a lower chemical affinity for the electrolyte ions. The effect of surface modifications is a decrease in pseudo-capacitance and a lower specific surface area available for the double-layer capacitance. Moreover, it is also likely that poor wettability of surfaces of the CMK-3B hinders the dispersion of carbon particles in the binder (Nafion ionomer) during the electrode preparation. Thus, the hydrophilic functional groups that have been introduced in the carbon from the carbonization of the oxygen-rich precursor (sucrose) [20, 36] have an important function in the improvement of the capacitive properties.

3.3. Electrochemical impedance spectroscopy (EIS) studies of carbon materials

Electrochemical impedance spectroscopy (EIS) is an important analytical technique and is used to get information about the characteristic frequency response of supercapacitors and the capacitive phenomena occurring in the electrodes.

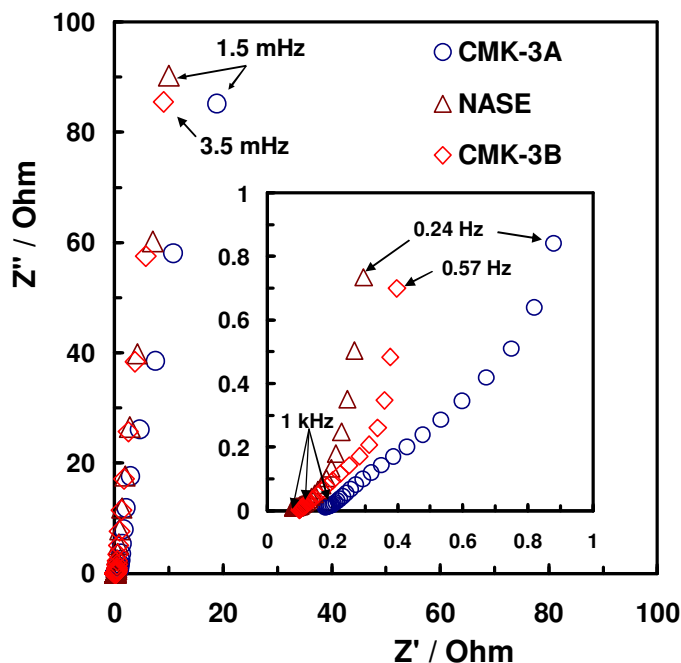The Nyquist impedance plots of the different capacitors are reported in Figure 5.

Figure 5. Nyquist plot of supercapacitors with CMK-3A, CMK-3B, and NASE carbons. The inset shows the high frequency region of impedance.

The inset in the figure shows the impedance behaviour at high frequencies of the capacitors with different carbon materials. The experimental points have a slope of 45° in the region with a higher frequency that is a consequence of the typical distributed resistance of porous carbon electrodes. At lower frequencies, the plots assume a shape close to that of an ideal capacitor and the points are almost dispersed in a vertical line. At high frequencies, the resistance characteristics of the different supercapacitors are expressed by the so-called electric series resistance (ESR), which include the electrolyte resistance, the collector/electrode contact resistance, and the electrode/electrolyte interface resistance. For the supercapacitors studied, the values of ESR are 0.8, 0.44, and 0.36 Ω cm^2 for CMK-3A, CMK-3B, and NASE, respectively. The ESR of the supercapacitor with CMK-3A carbon in the electrodes is higher than the other carbons (NASE and CMK-3B), because it has a lower degree of graphitization and/or it has more surface functional groups, which decrease the electronic conductivity of the material, even if these facilitate the carbon wettability extending from the electrodes/electrolyte

interfaces [37-38]. Besides, it is likely that the surface functional groups, in the CMK-3A sample supply additional electric charge by pseudo-capacitive processes due to redox reactions. The distortion of rectangular shape of voltammogram of CMK-3A carbon (Figure 4) for cell voltages from 0 to 0.3 V, for positive and negative currents (charge/discharge phases), is a clear indication of the presence of these processes. It is not possible to give an exact quantification of such pseudo-capacitance compared to the overall capacitance, but it should be much higher than 10% of total measured capacitance, as is reported in the current literature [39-40].

When the difference in the cyclic voltammetry experiments is considered, the analysis of the Nyquist plot of Figure 5 does not give any clear information about pseudocapacitive processes (from redox reactions) occurring in the electrodes.
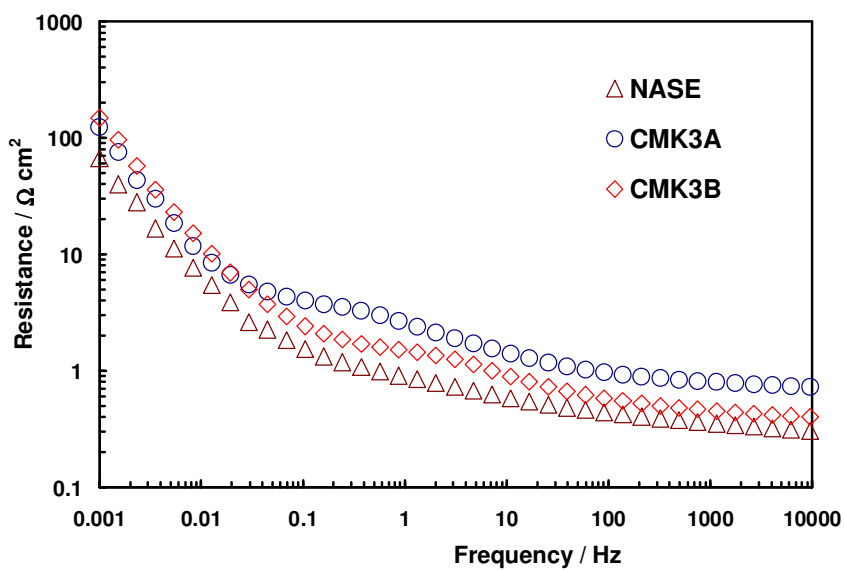

Figure 6. Resistance behaviour as a function of frequency for CMK-3A, CMK-3B, and NASE carbons.

Figure 6 shows the resistance behavior of the different capacitors as a function of frequency. Initially, in the high frequency region, the main resistances are those due to the Nafion electrolyte, which is 0.16 Ω cm^2, and that of two electrodes. In the middle frequency range (e.g., from mHz to Hz), the predominant resistances are those due to the penetration of ions and the electric signal through pores of carbon. The surface functional groups favor the transport of ions in small carbon pores using chemical affinity as is demonstrated from the behavior of the resistance as a function of frequency in Figure 6 for the capacitor with CMK-3A carbon. In fact, the capacitor with CMK-3A has the highest resistance at a high frequency, compared to capacitors with other carbons. Whilst at the lower frequency, the resistance of the CMK-3A capacitor is comparable to CMK-3B and NASE capacitors. This occurs because the CMK-3A carbon provides a more wettable surface and better transport of electrolyte ions, which is more evident at lower frequencies.

Figure 7 shows the trend in specific capacitances as a function of frequency for the different supercapacitors. At a frequency of 1 mHz, the capacitance values for CMK-3A, NASE, and CMK-3B are 132, 80.5, and 55.3 F g^{-1}, respectively, while, the double-layer capacitance per unit of surface area for the CMK-3A is 12.05 $\mu F\ cm^{-2}$. This capacitance is higher than that of NASE activated carbon, 5.3 $\mu F\ cm^{-2}$, and that of CMK-3B, 7.3 $\mu F\ cm^{-2}$. However, one disadvantage is that the capacitance of CMK-3A is influenced more by the frequency, which is in agreement with the results discussed for the cyclic voltammetry experiments.
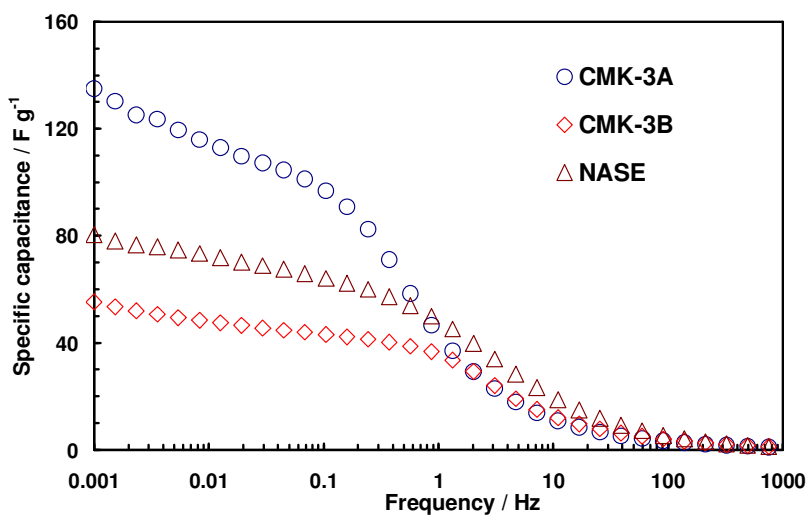

Figure 7. Specific capacitance (F g^{-1}) as a function of frequency carbon-based supercapacitors. The capacitance (F g^{-1}) is normalized for the weight of carbon materials in a single electrode.

The value of capacitance for the CMK-3A-based supercapacitor, 132 F g^{-1}, is higher than that reported by Zhou [37] for the same type of CMK-3 carbon, measured in a three electrode cell using the $LiPF_6$/ethylene carbonate (EC) electrolyte/solvent system. The capacitances Zhou reported [37] varied from 60-90 F g^{-1}, whereas Vix-Guterl et al. [20] reported capacitance values in 1M H_2SO_4 and in Et_4NBF_4 of 167 and 93 F g^{-1}, respectively. In literature reviews [1-6] it is well known that higher specific capacitances are generally obtained using aqueous electrolytes than non-aqueous electrolytes. However, the advantage of the capacitor with non-aqueous organic electrolytes is that it is possible to obtain a higher energy density ($E_{max} = 1/2\ CV^2$) for a wide range of voltage stabilities. However, the characteristic performances of our mesoporous carbon-based solid-state supercapacitor and the relative study are new, in this specific field of research.

In a recent paper, Centeno et al. [41] reported capacitance values for mesoporous carbons as high as 150-200 F g^{-1} in an aqueous solution of H_2SO_4, whereas values of less that 100 F g^{-1} were recorded for mesoporous carbon materials in a non-aqueous electrolyte.

The capacitance values reported here and the comparison with those discussed in the literature [20, 37-41], confirm that mesoporous carbon is a very interesting material that may be used as potential substitute, in the near future for the traditional activated carbons in the preparation of high performance supercapacitors.

One finding of this work is that we have shown that potential improvements of supercapacitor features could be achieved by: a) increasing the specific surface area and optimizing the pores structure; and b) a better understanding of the ions transport process through carbon pores. However, because there are many influences between different parameters, for example, between surface functional groups, pores structure, and surface wettability, a correlations between the carbon material's properties and the capacitance performance of the supercapacitors can not be permitted. Therefore, we believe that no axiom can be confidently used to predict the capacitance behavior of different carbon materials, when they are studied in different types of supercapacitors.

4. CONCLUSIONS

In this study, we have reported the synthesis of mesoporous CMK-3 type carbon using SBA-15 silica as a template material. The successful synthesis and the characteristics of pore structures of mesoporous carbons have been studied using different physico-chemical characterizations. It was found that the synthesized carbon materials were characterized by a highly ordered hexagonal structure with a rod-like domain and by a main pore size of about 3.6 nm. Two different carbon samples (CMK-3A and CMK-3B) obtained at different carbonization temperatures, 850 and 900 °C, had different properties. In fact, the two mesoporous carbons had remarkable differences with regard to the specific surface area and surface functional groups, which were reflected by different electrochemical behaviours. The supercapacitors using the mesoporous nano-structured carbon carbonized at 850 °C (CMK-3A) had a high specific capacitance, 132 F g^{-1}, compared to than of CMK-3B, 55.3 F g^{-1}, which was carbonized at 900 °C, and compared to that of a reference activated carbon (NASE), 80.5 F g^{-1}. The lower specific capacitance of the supercapacitor with the carbon treated at 900 °C (CMK-3B) compared to than with the carbon treated at 850 °C (CMK-3A) is ascribed to the former carbon having lower pseudo-capacitance and a smaller amount of surface functional groups.

The highest specific capacitance of the supercapacitor, with the CMK-3A carbon, may be explained on the basis of concomitant positive influences as: a) the mesoporous structure of carbon, b) the surface wettability due to surface functional groups, and c) the additional pseudo-capacitance derived from redox processes. Nevertheless, one disadvantage of this carbon is that higher electronic resistance has been determined from the surface functional groups. The results of this study demonstrate that mesoporous carbons may be considered very promising materials for the development of high performance in the design and development of lightweight and flexible polymer electrolyte-based supercapacitors.

References

1. B.E. Conway, in "Electrochemical Supercapacitors: Scientific Fundamental and Technological Applications", Kluwer Academic - Plenum Publishers New York (1999).

2. P. Simon, Y. Gogotsi, *Nature Mater.* 7 (2008) 845.
3. R. Kotz, M. Carlen, *Electrochimica Acta* 45 (2000) 2483.
4. A.G. Pandolfo, A.F. Hollenkamp, *J. Power Sources* 157 (2006) 11.
5. E. Frackowiak, F. Beguin, *Carbon* 39 (2001) 937.
6. M. Jayalakshmi, K. Balasubramanian, *Int. J. Electrochem. Sci. 3* (2008) 1196.
7. S.H. Kim, Y.I. Kim, J.H. Park, J.M. Ko, *Int. J. Electrochem. Sci.* 4 (2009) 1489.
8. Y-J. Kim, Y. Masutzawa, S. Ozaki, M. Endo, and M.S. Dresselhaus, *J. Electrochem. Soc.* 151 (2004) E199.
9. R. Saliger, U. Fischer, C. Herta, J. Fricke, *J. Non-Cryst Solids* 225 (1998) 81.
10. X. Zeng, D. Wu, R. Fu, H. Lai, *Mater. Chem. Phys.* 112 (2008) 1074.
11. A.B. Fuertes, G. Lota, T.A. Centeno, E. Frackowiak, *Electrochimica Acta* 50 (2005) 2799.
12. E. Lust, A. Janes, M. Arulepp, *J. Solid State Electrochem.* 8 (2004) 488.
13. Y.J. Huai, X.B. Hu, Z.J. Lin, Z.H. Deng, J.H. Suo, *Mater. Chem. Phys.* 113 (2009) 962.
14. F. Lufrano, P. Staiti, and M. Minutoli, *J. Power Sources* 124 (2003) 314.
15. F. Lufrano, P. Staiti, and M. Minutoli, *J. Electrochem. Soc.* 151 (2004) A64.
16. F. Lufrano, P. Staiti, *Electrochimica Acta* 49 (2004) 2683.
17. P. Staiti, F. Lufrano *Electrochimica Acta* 53 (2007) 710.
18. H. Zhou, S. Zhu, M. Hibino, I. Honma, M. Ichihara, *Adv. Mater.* 15 (2003) 2107.
19. D.S. Yuan, J. Zeng, J. Chen, Y. Liu, *Int. J. Electrochem. Sci.* 4 (2009) 562.
20. C. Vix-Guterl, E. Frackowiak, K. Jurewicz, M. Friebe, J. Parmentier, F Béguin, *Carbon* 43 (2005) 1293.
21. H. Tamai, M. Kouzu, M. Morita, H. Yasuda, *Electrochem. Solid-State Lett.* 6 (2003) A214.
22. Y. Yamada, O. Tanaike, T. T. Liang, H. Hatori, S. Shiraishi, A. Oya, *Electrochem. Solid-State Lett.* 5 (2002) A283.
23. S. Yoon, J. Lee, T. Hyeon, S.M. Oh, *J. Electrochem. Soc.* 147 (2000) 2507.
24. R. Ryoo, S. H. Joo, S. Jun, *J. Phys. Chem.* B 103 (1999) 7743.
25. S. Jun, S.H. Joo, R. Ryoo, M. Kruk, M. Jaroniec, Z. Liu, T. Ohsuna, O. Terasaki, J. *Am. Chem. Soc.*, 122 (2000) 10712.
26. D. Zhao, J. Feng, Q. Huo, N. Melosh, G.H. Fredirckson, B.F. Chemlka, D.G. Stucky, *Science* 279 (1998) 548.
27. S. H. Joo, S. J. Choi, I. Oh, J. Kwak, Z. Liu, O. Terasaki, R. Ryoo, *Nature,* 412 (2001) 169.
28. M. Kruk, M. Jaroniec, J. Choma, *J. Colloid Interface Sci.*, 192 (1997) 250.
29. E.P. Barrett, L.G. Joyner, P.P. Halenda, *J. Am. Chem. Soc.* 73 (1951) 373.
30. A.B. Fuertes, *Microporous Mesoporous Mater.* 67 (2004) 273.
31. Lu, A. Kiefer, W. Schimdt, F. Schüth, *Chem. Mater.* 16 (2004) 100.
32. M. Endo, T. Maeda, T. Takeda, Y.J. Kim, K. Koshiba, H. Hara, M.S. Dresselhaus, *J. Electrochem. Soc.* 148 (2001) A910.
33. S. Shiraishi, H. Kurihara, L. Shi, T. Nakayama, A. Oya, *J. Electrochem. Soc.* 149 (2002) A855.
34. O. Barbieri, M. Hahn, A. Herzog, R. Kotz, *Carbon* 43 (2005) 1303.
35. C.-H. Kim, S.-I. Pyun, H.-C. Shin, *J. Electrochem. Soc.* 149 (2002) A93.
36. C. Vix-Guterl, S. Saadallah, K. Jurewicz, E. Frackowiak, M. Reda, J. Parmentier, J. Patarin, F. Beguin, *Mater. Sci. Eng.* B 108 (2004) 148.
37. H. Zhou, S. Zhu, M. Hibino, I. Honma, *J. Power Sources* 122 (2003) 219.
38. T.A. Centeno, M. Sevilla, A.B. Fuertes, F. Stoekli, *Carbon* 43 (2005) 3012.
39. Alonso, V. Ruiz, C. Blanco, R. Santamaria, M. Granda, R. Menendez, S.G.E. de Jager, *Carbon* 44 (2006) 441.
40. S.R.S. Prabaharan, R. Vimala, Z. Zainal, *J. Power Sources* 161 (2006) 730.
41. T.A. Centeno, F. Stoekli, *Electrochimica Acta* 52 (2006) 560.